Interruption of conjugations of polyacetylene chains

Péter R. Surján
Central Research Institute for Chemistry, Hungarian Academy of Sciences, P.O. Box 17, H-1525 Budapest, Hungary and Chinoin Research Centre, Budapest, Hungary

Hans Kuzmany
Institut für Festkörperphysik der Universität Wien, A-1090 Wien, Austria and Ludwig Boltzmann Institut für Festkörperphysik, Wien, Austria
(Received 4 September 1985)

The interruption of conjugations in polyacetylene, $(CH)_x$, is studied with the use of a tight-binding model Hamiltonian capable of describing various chain defects in $(CH)_x$. The effect of twisting, local impurities, *cis* segments, chain bending, and attached side groups on electronic transition energies and intensities is investigated. Rotations around "double" C=C bonds of the conjugated $(CH)_x$ chain lead to the formation of a soliton-antisoliton pair. To study the effect of sp^3-type defects or crosslinks in polyacetylene, all-valence-electron model calculations are performed for smaller model systems. It is found that rotations around single C—C bonds, carbonyl side groups, and sp^3-type chain defects lead to a partial interruption of the conjugation. To account for experimental findings from, e.g., resonance Raman scattering, such types of defects must be present in a relatively high concentration which is possible only if certain domains with a very high density of defects exist in polyacetylene while keeping the average defect concentration at a low value.

I. INTRODUCTION

Polyacetylene continues to attract considerable interest from physicists and chemists, particularly in the area of basic research.[1] This is due to its very simple chemical structure and its high crystallinity.[1(b)] In addition, the high metalliclike conductivity after doping and unusual magnetic properties stimulate research work. As it turns out, a detailed understanding not only of the structure of the pristine material but also of the defects along the chains is required. This holds true not only for problems concerned with conductivity, where a strong interaction between the intercalated species and the polymer and the relaxation of the chain is expected to be important, but also for spin motion along the chain and for problems concerned with electronic transitions like optical absorption or Raman scattering. In particular, the experimental results of the unusual dispersion effect of the resonance Raman lines of *trans*-polyacetylene suggested a particle-in-a-box—type behavior of the π electrons on the chains. Thus, the latter are assumed to be statistically interrupted by defects[2–6] and the physical properties of the polymer may be described by a distribution of chains or segments of various lengths. The anomalous resonance Raman effect (*vide infra*) can be described quantitatively within this model, and the fitting of calculated Raman lines and Raman intensities to experimental results facilitates evaluation of the sample-specific distribution function for the segment lengths.

The resonance Raman effect of *trans*-polyacetylene is anomalous in the sense that the shape and position of several Raman lines changes dramatically with the frequency of the exciting laser. Line shifts up to 60 cm^{-1} for laser quantum energies between 1.8 and 3 eV have been observed. The description of this effect is based on a photoselective resonance process. Red and blue laser light excites resonantly only the specific part of the polymer which is accommodated in long and short segments, respectively. Thus, for the resonance excitation with the blue laser electronic transition energies of the order of 3 eV are required which are characteristic π-π^* transition energies for chains with five double bonds. Accordingly, so far complete interruption of the π-electronic system on the chain into segments of various lengths was assumed phenomenologically.

The purpose of this paper is to give a realistic and physical interpretation of the term "interruption of conjugation," rather than a sophisticated quantum-chemical treatment of the system. Thus, by using simple models, we study the electronic structure of polymer chains containing various types of well-characterized defects on the conjugation. We investigate to what extent these defects interrupt the conjugation without interrupting the chain, and to what extent these interruptions lead to physical properties equivalent to a complete chain interruption. The underlying models and methods are specified in Sec. II. Numerical calculations were performed on a generalized Hückel or on the "spectroscopic complete neglect of differential overlap" (CNDO/S) level. Chain end effects are automatically included. In Sec. III the results on electronic excitation energies and transition moments are presented for various kinds of conjugation interruptions. The following defects will be discussed: several types and arrangements of twists on a polyene chain, chain bending and local impurities, *cis* segments in a *trans* chain, side-groups and crosslinks, and relaxation of bond lengths. Preliminary results of these investigations have been published recently.[7]

II. METHOD OF CALCULATION

A. Generalization of the Hückel model

1. Model Hamiltonian

In order to describe the π-electron structure of finite, long, pure polyene chains the simple Hückel tight-binding Hamiltonian of the form

$$H=\sum_{\mu,\sigma}\beta_\mu(a^\dagger_{\mu,\sigma}a_{\mu+1,\sigma}+\text{H.c.}) \tag{2.1}$$

is appropriate with open end boundary conditions. In Eq. (2.1) $a^\dagger_{\mu,\sigma}$ creates an electron on the atomic orbital (AO) χ_μ with spin σ, while β_μ is the resonance integral between the AO's χ_μ and $\chi_{\mu+1}$. The AO's are represented by $2p_z$ Slater-type orbitals (STO's),[8] one on each carbon. Only the π electrons are treated explicitly. This π-electron Hamiltonian is diagonalized by the unitary transformation

$$\psi_i=\sum_\mu c_{i\mu}\chi_\mu\ , \tag{2.2}$$

which leads to

$$H=\sum_{i\sigma}\varepsilon_i\psi_i^+\psi_i^-\ ,$$

where ψ_i^+ (ψ_i^-) create (annihilate) an electron on the molecular orbital (MO) ψ_i of Eq. (2.2), and the ε_i are the orbital energies. The total π-electron energy is given by

$$E=\sum_i g_i\varepsilon_i\ , \tag{2.3}$$

g_i being the occupation number of the MO ψ_i. Excitation energies corresponding to the $i\rightarrow j^*$ transition are obtained as

$$\Delta\varepsilon_{i\rightarrow j^*}=\varepsilon_{j^*}-\varepsilon_i\ . \tag{2.4}$$

In the present study we shall also pay attention to the intensities of the electronic transitions, which are characterized by the transition moments ρ_{ij^*}. The latter can be evaluated in the dipole velocity formalism:

$$\rho_{ij^*}=\sqrt{2}\Delta\varepsilon_{ij^*}^{-1}\langle\psi_i\,|\,\hat{\nabla}\,|\,\psi_{j^*}\rangle \tag{2.5}$$

(in atomic units), where the factor $\sqrt{2}$ arises from spin adaptation and the matrix elements of the gradient operator $\hat{\nabla}$ can be obtained by inserting the expansion of Eq. (2.2):

$$\langle\psi_i\,|\,\hat{\nabla}\,|\,\psi_{j^*}\rangle=\sum_{\mu,\nu}c_{i\mu}c_{j^*\nu}\nabla_{\mu\nu}\ .$$

As it is consistent with the spirit of the Hückel theory, the $\nabla_{\mu\nu}$ integrals over AO's have been evaluated in the nearest-neighbor approximation. The remaining matrix elements are calculated over carbon $2p_z$ STO's at the actual bond distances. We note that numerical checks showed the importance of second-neighbor gradient integrals to be negligible.

The Hamiltonian of Eq. (2.1) can describe only pure $(CH)_x$ chains. In order to describe various defects along the chain, it is necessary to generalize our model. We apply the following model Hamiltonian:

$$H=\sum_{\mu,\sigma}[\alpha_\mu a^\dagger_{\mu\sigma}a_{\mu\sigma}+\beta^0_\mu(r_\mu)(\cos\varphi_\mu)(a^\dagger_{\mu\sigma}a_{\mu+1,\sigma}+\text{H.c.})]+\sum_\mu f_\mu(r_\mu)\ . \tag{2.6}$$

The first term of Eq. (2.6) describes diagonal disorder induced by impurities on the chain. The second term is capable of describing off-diagonal disorder induced by twists of the chain or relaxation phenomena (electron-phonon coupling), while the last term considers contributions from the σ electrons in a phenomenological way, permitting us to describe relaxation effects. The factor $\cos\varphi$ at the resonance integral takes into account the decrease of the β integral upon twisting the chain around the corresponding bond by an angle of φ. The σ-core potential in Eq. (2.6), $f_\mu(r_\mu)$, is determined in the spirit of the model by Longuett-Higgins and Salem (LS).[9] Accordingly,

$$f_\mu(r_\mu)=2\beta^0_\mu(r_\mu)(a-1.5+r_\mu)/0.15\ , \tag{2.7}$$

and the resonance integral is taken as an exponential function of the corresponding bond distance r_μ:

$$\beta^0_\mu(r_\mu)=-A\exp(-r_\mu/a)\ , \tag{2.8}$$

where a and A are parameters in units of Å and eV, respectively. The parameters are chosen to recover Coulson's linear relationship between r_μ and the π-electron bond order P_μ at optimum geometries in the form

$$r_\mu=1.5-0.15P_\mu\ . \tag{2.9}$$

The LS method closely by parallels the Su-Schrieffer-Heeger (SSH) model[10] for $(CH)_x$. The differences are that in the SSH Hamiltonian the $\beta(r)$ function of Eq. (2.8) is expanded in a Taylor series up to the first order only, and the usual parametrization violates the Coulson relationship of Eq. (2.9). This feature may lead to improper bond lengths and thus to incorrect values for transition moments. For this reason we prefer to use the LS-type Hamiltonian, which has previously been applied in studying geometry distortions due to soliton phase kinks in polyacetylene.[11,12]

2. Choice of the empirical parameters

The original parametrization of the LS model,[9] fitted to the force constants of ethylene and benzene, leads to resonance integrals unsuitable for spectroscopic purposes. Therefore we reparametrized the LS model in the following manner. To describe the pristine chain, we took

$$\beta_>=-3.35\ \text{eV}$$

and

$$\beta_<=-2.65\ \text{eV}$$

for the alternating double and single bonds, respectively. These values reproduce the infinite gap of *trans*-$(CH)_x$, 1.4 eV, and the lowest allowed π-π^* electronic transition of butadiene, 4.5 eV. Diagonalizing the electronic part of the Hamiltonian (2.6) for an infinite, pure regularly alternating chain (i.e., taking $\alpha_\mu=0$ and $\varphi_\mu=0$ for all μ), we obtain for the π-electron bond orders $P_<=0.438$ and $P_>=0.818$. This corresponds to the equilibrium geometry $r_>=1.434$ Å and $r_<=1.377$ Å according to Coulson's relationship of Eq. (2.9). The bond lengths thus obtained, together with the resonance integral values given above, determine the parameters A and and a in Eq. (2.8): $A=965.67$ eV, $a=0.243$ Å.

B. CNDO/S calculations

The model Hamiltonian introduced in Sec. II A is unable to account for the mixing of σ- and π-type orbitals. Such mixing occurs if the system in question is not planar, e.g., if twists or sp^3-type defects are considered in $(CH)_x$. In order to estimate the role of σ-π mixing in transition energies and intensities, and also to perform calculations when the σ-π separation is inadequate, we used the semiempirical CNDO/S method[13] in some cases. This is an all-valence-electron self-consistent-field (SCF) method taking electron-electron interaction explicitly into account. Relative to the Hückel-type studies, the CNDO/S method requires considerably increased amount of computation; thus only shorter chains have been treated by this approach. We note that the importance of electron-electron interaction in $(CH)_x$ has also been stressed recently by Soos and Stafström[14] on the basis of Hubbard- and Pariser-Parr-Pople— (PPP) type models; the CNDO/S is superior to these since it accounts also for the σ-π interaction. In the following we give a short description of the basic features of the CNDO/S method, because it has been rarely used in solid-state calculations.

The ground-state wave function is represented by a Slater determinant of occupied valence MO's. The latter are obtained by diagonalizing an empirically parametrized Fockian self-consistently. The underlying basis set consists of the valence AO's of the atoms forming the molecule and is assumed to be orthonormalized. In any integral, the zero-differential-overlap (ZDO) condition is used; that is, any integral containing the product of two different AO's is taken to be zero. However, resonance integrals entering the off-diagonal elements of the Fockian are taken to be proportional to the corresponding overlap matrix elements. The factor of this proportionality, the one-center repulsion integrals, and the ionization potentials of atoms entering the diagonal elements of the Fockian are handled as empirical parameters. Two-center electron repulsion integrals are evaluated by means of the Mataga-Nishimoto formula.[15]

The excited-state wave function for a singlet state is given by

$$|\Psi_K\rangle=\frac{1}{\sqrt{2}}\sum_{i,j^*}C_{ij^*}^K(\psi_{j^*\alpha}^+\psi_{i\alpha}^-+\psi_{j^*\beta}^+\psi_{i\beta}^-)|\Psi_0\rangle\ ,$$

where $|\Psi_0\rangle$ is the ground-state wave function, α and β stands for spin labels, and the C_{ij}^K coefficients are determined variationally. That is, a configuration-interaction (CI) procedure is performed including single excitations.

The CNDO/S method can be considered as a generalization of the π-electron Pariser-Parr-Pople method[16] to the all-valence-electron level. It has been widely used to calculate optical properties of various molecules.[17]

It is to be noted that the Hückel- and PPP-type Hamiltonians possess the so-called electron-hole symmetry if no impurity (diagonal perturbation) is considered. That is, these Hamiltonians are invariant under a transformation which converts the electrons and holes into each other. As a consequence, the energies of the occupied and virtual levels in these models have the same absolute value if the Fermi energy is chosen to be zero. This is, of course, far from being true in reality and represents an oversimplification in the Hückel and PPP approaches. The CNDO model, however, does not necessarily possess electron-hole symmetry, due to the presence of second-neighbor and σ-π interactions in nonplanar structures. This feature permits us to obtain much more realistic orbital energies for these systems.

III. RESULTS

A. Chain twisting

1. Single twist

For the study of the chain twisting the Hamiltonian of Eq. (2.6) with $\alpha_\mu=f_\mu(r_\mu)=0$ for all μ was used. That is, no diagonal disorder is considered and the role of electron-phonon coupling is neglected. The effect of a rotation around a particular C—C bond μ is considered as a partial interruption of the conjugation *via* decreasing the overlap of the corresponding $2p_z$ orbitals. This is expressed by the factor $\cos\varphi_\mu$ in our model Hamiltonian. It can be seen immediately from the Hamiltonian (2.6) that $\varphi_\mu=90°$ interrupts the conjugation completely at the position μ and thus separates the chain into two parts. Mixing between σ and π orbitals is neglected by Eq. (2.6). As will be shown by the CNDO/S calculations below, this is a good approximation for $\varphi\lesssim 80°$.

The results of a calculation as obtained by diagonalizing our Hückel-type model Hamiltonian for a $(CH)_6$ chain are shown in Figs. 1(a) and 1(b) as circles, for optical transition energies and transition moments, respectively. The solid lines are guidelines for the eye. Here and in the following the MO's identifying the transitions are counted from the top of the valence band (π band) and from the bottom of the conduction band (π^* band).

In order to demonstrate the reliability of the Hückel-type model in studying the effect of twisting, we have compared the Hückel-type results based on the Hamiltonian (2.6) with those obtained by the more sophisticated valence-electron SCF-CI-CNDO/S method. The results presented in Figs. 1(a) and 1(b) (crosses) show very good agreement for twists up to 60°—80°. At about 90° the assignment of the transitions by the CNDO/S wave function becomes difficult due to the increased σ-π mixing and also due to the considerably increased mixing of pure excitations in the CI calculation. The Hückel-type transi-

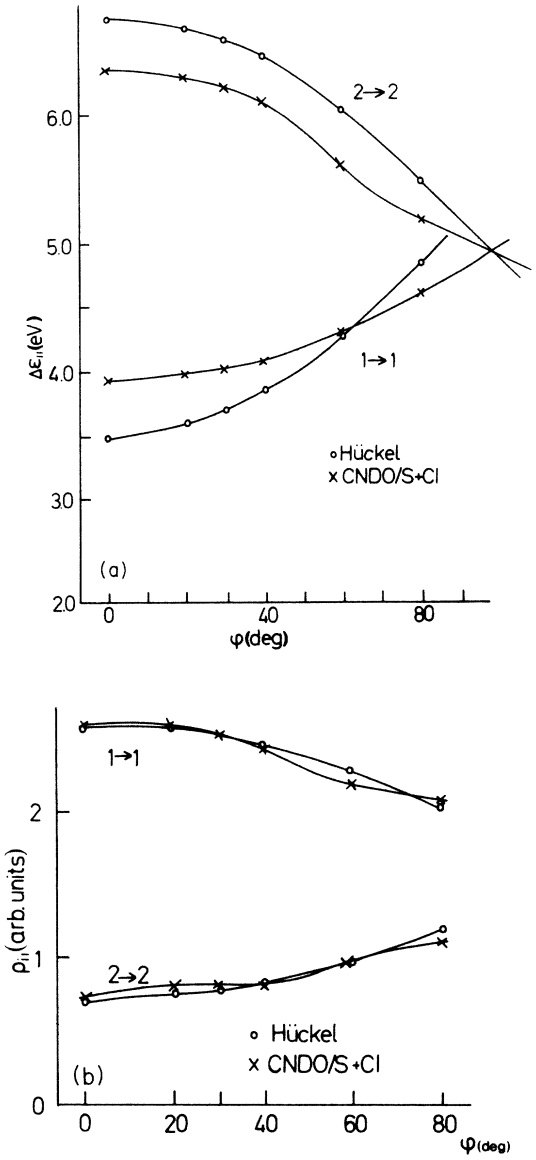

FIG. 1. CNDO/S-CI versus Hückel results on transitions for various twist angles φ in a $(CH)_6$ chain. (a) Transition energies; the Hückel results are scaled by 1.4. (b) Transition moments in arbitrary units; the Hückel results are scaled by 2.0.

tion energies become degenerate at 90° if the twist is in the middle of the chain. This is not exactly the case in the CNDO/S model, where the degeneracy is split due to σ-π interaction. However, it is seen that the simple Hückel model is useful in studying the effect of twists on low-lying π-π^* transitions; only the conclusions concerning twists around 90° should be handled with some care.

In the following, the Hückel-type model Hamiltonian of Eq. (2.6) will be used, which allows us to treat long polyene chains with reasonable effort. The more elaborate CNDO/S calculations will be performed only in cases when the purely π-electron picture is inadequate (see Sec. III C).

An immediate extension of the results presented above is the study of a single twist of angle φ on the electronic properties of an extended chain with N double bonds. The twist is assumed in the middle of the chain. Figure 2 shows the first three occupied orbital energies ε_i for three different values of φ as a function of the chain length N. The odd-numbered transition energies increase considerably with increasing twist angles, particularly for short chains. The energies of even-numbered vertical transitions behave in an opposite manner.

Figure 3 shows the influence of similar twists on transition moments ρ_{ii^*}. The larger the twist, the less intense the first transition, and the more intense the second vertical transition. This is in agreement with the observed monotonic relationship between transition energies and transition moments.[6,18] We note, however, that for the 90° twist, due to the degeneracy of the corresponding states, $\rho=(\rho_{11^*}^2+\rho_{22^*}^2)^{1/2}$ is the only physically relevant quantity.

The investigation of the influence of the position of a single twist on the electronic ground-state energy revealed an interesting result. Figure 4 shows the total energy $E_\sigma+E_\pi$ of a chain as a function of the location μ of a twist of 40°. Apparently, the rotation is easier around a bond near the chain ends. Positions in the interior of the chain are energetically equivalent if an equidistant geometry is used (crosses). This result holds true even for a relaxed geometry (open circles) and is the opposite of the case of soliton-type defects, for which the potential energy is shown schematically in the top of the figure.

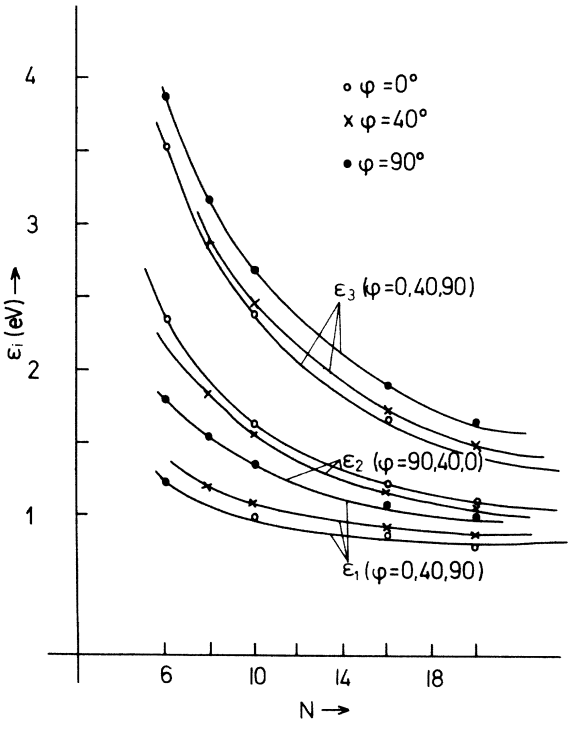

FIG. 2. Orbital energies ε_i for various twist angles φ as functions of the chain length N (number of double bonds).

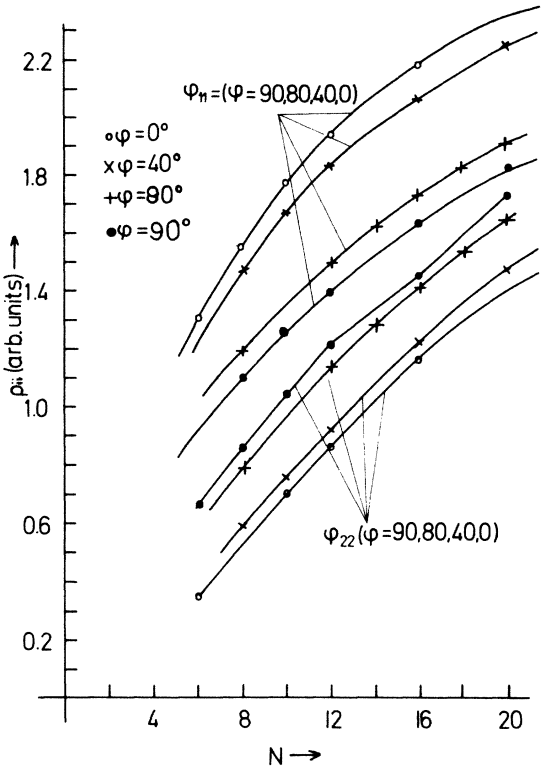

FIG. 3. Transition moments ρ_{ii} for vertical transitions for various twist angles φ as a function of the chain length N.

2. *Accumulation of twists*

The results of Fig. 2 show that even a strong single twist on a long chain does not strongly increase the electronic transition energies. In a realistic case of the polyacetylene chain, the effect of a statistical distribution of twists may sum up to an opening of a large gap. Thus, we have performed a series of calculations containing ten twists of 40° at randomly selected places. The results are plotted in Figs. 5(a) and 5(b) as a probability histogram for the five lowest vertical transitions. The twists on the chain obviously increase the transition energies and decrease the transition moments. In addition, the evaluated energies depend on the selected places for the twists. However, the total range of transition energies for a particular transition covers only about 0.4 eV. Thus, the increase of the transition energy is not strong enough to reach the range of 3 eV for the first transition in a 50-double-bond chain.

We may ask how many twists we have to accommodate on the chain in order to get close to 3 eV for the first transition. Figure 6 shows the increase of the lowest excitation energy as a function of the number of 60° twists (n) on the $(CH)_{100}$ chain. It is seen that one has to assume a concentration of ~ 20 twists of 60° in order to reach ~ 2.7 eV for $\Delta\varepsilon_{1\to 1^*}$.

We have also studied a helical or wormlike chain. Twists of equal size are accommodated in this case on n consecutive C—C single bonds in order to establish a total twist of 90°. Figure 7 shows the change of the first four orbital energies as a function of the individual twist angle φ (i.e., n twists of $\varphi=90°$) for a $(CH)_{60}$ chain. The single 90° twist in the middle of the chain ($n=1$) leads to a degeneracy of the two consecutive states. However, for smaller individual twists (larger values of n) the increase of $\Delta\varepsilon$ is small. For $n=9$ twists of 10° each, one has, e.g., nearly no influence on the electronic states. The changes in the electronic transition moments were again found to be correlated in the usual way to the changes in the transition energies.

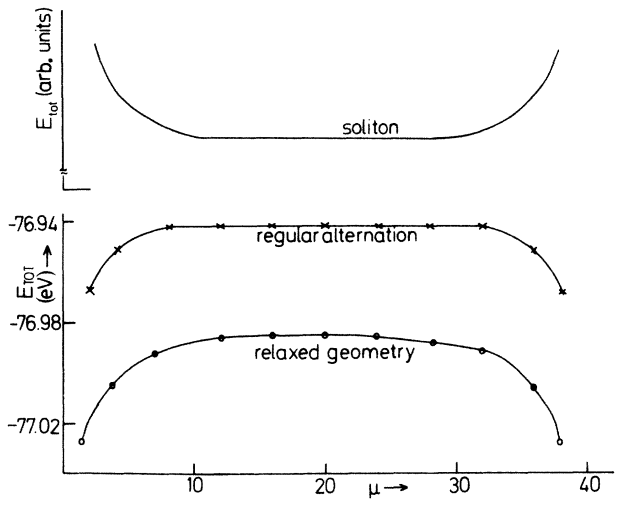

FIG. 4. Total $\sigma+\pi$ energies for a $(CH)_{40}$ chain as a function of the place μ of a twist of 40°, for regularly alternating geometry (×) and for energy optimized bond lengths (○). The top curve shows the energy of a soliton schematically.

B. Twisting around double bonds

In the above study we have considered only rotations around a "single" C—C bond in the polyene chain. In reality, there are no pure single and double bonds in $(CH)_x$ as a consequence of the strong conjugation. Therefore it is important to check the possibility for a rotation around a "double" C=C bond as well.

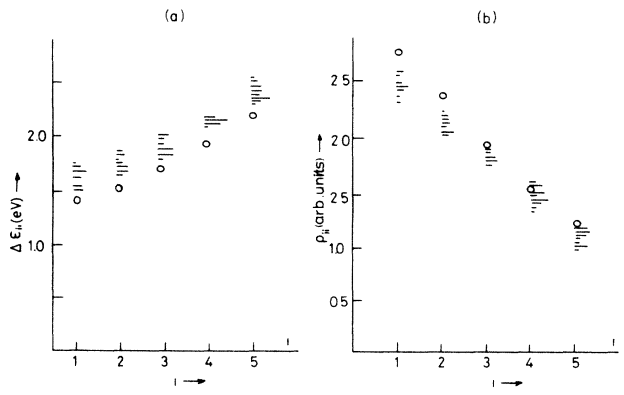

FIG. 5. Probability histogram for a $(CH)_{100}$ chain with ten twists at randomly selected places. (a) Transition energies; (b) transition moments for the five lowest vertical transitions i (—) and for the undisturbed chain (○).

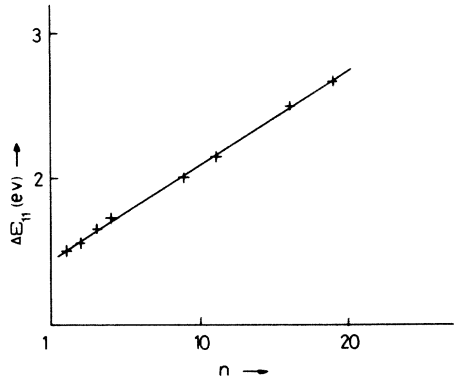

FIG. 6. The lowest transition energy ($\Delta\varepsilon_{11}$) of a $(CH)_{100}$ chain as a function of the number of 60° twists (n) having an equidistant distribution along the chain.

In general, internal rotations around pure single bonds are almost free, the corresponding energy barrier being a few kcal/mol, while rotations around true double bonds are hindered. For instance, the barrier to the internal rotation in ethylene is ~60 kcal/mol.[19]

In the case of polyacetylene, one can assume that the value of the barrier to a rotation around a particular bond i, V_i, depends on the π-electron bond order P_i of that bond. As a first approximation, this dependence can be taken as linear: $V_i = a + bP_i$. Fitting the parameters a and b to the experimental barriers of ethylene ($P_i = 1.0$, $V_i = 63$ kcal/mol $= 2.7$ eV) and butadiene ($P_i = 0.45$ with our β's, $V_i = 5.1$ kcal/mol $= 0.22$ eV), we obtain the barrier-bond order relationship in the form

$$V_i = -1.8 + 4.5P_i \quad \text{(in eV)} . \tag{3.1}$$

For long polyene chains, we have $P_< = 0.438$ and $P_> = 0.818$ (cf. Sec. II B). By Eq. (3.1), this leads to an estimation for the barriers to rotation ~0.2 eV around "single" C—C bonds, as opposed to ~1.9 eV around "double" C=C bonds in the $(CH)_x$ chain.

If one allows the geometry of the chain to relax upon twisting, i.e., one deals also with the σ part of the model Hamiltonian of Eq. (2.6), one finds a much larger relaxation energy for a rotation around a "double" C=C bond

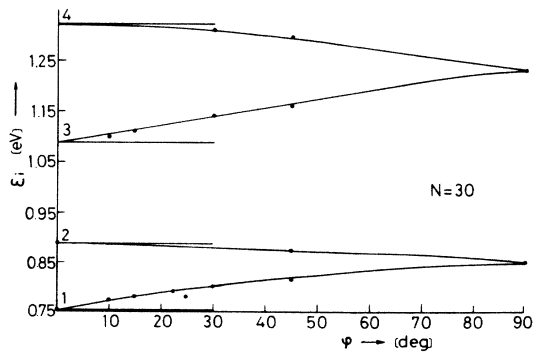

FIG. 7. Orbital energies in a $(CH)_{60}$ chain containing a wormlike twist in the middle, as a function of the value for the individual twists.

than around a "single" C—C bond. This is quite natural since a twist around a double bond strongly influences the bond-length alternation: a soliton-antisoliton pair has been found when optimizing the geometry for a twist of an angle $\varphi \gtrsim 60°$ around a "double" bond. The relaxation energies upon the formation of this soliton-antisoliton pair were found to be comparable with the barrier to rotation around a double bond as estimated by Eq. (3.1). A similar mechanism for generating soliton-antisoliton pairs in $(CH)_x$ has been described recently by Gibson *et al.*;[20] in that study the rotation is supposed to be motivated by the presence of remanent *cis* units and thermal activation.

As to the transition energies of a chain possessing a twist around a double bond, the most important point is that, due to the presence of the soliton-antisoliton pair, one has two midgap states. This indicates that bond-length—relaxation effects tend to close the gap in this case. Accordingly, twists around "double" bonds are not responsible for explaining the increased excitation energy observed from resonance Raman experiments.

It is to be emphasized that rotations around single bonds in $(CH)_x$ require much less energy so they can be considered not only as excitations but also as defects of the $(CH)_x$ chain.

C. Inclusion of *cis* segments

cis segments can formally be obtained by considering a 180° rotation around the relevant C—C bond axis. The bond lengths and the corresponding overlaps do not change upon this rotation to a first approximation. Some non-nearest-neighbor integrals, however, would change, but, as we have checked numerically, their changes do not have any appreciable effect on the electronic structure because even the second-neighbor integrals are rather small themselves in any reliable parametrization. Another effect of the *cis-trans* isomerization is that the equilibrium, i.e., the energy-optimized bond lengths, slightly depend on this geometrical change.[21] This suggests use of different first-neighbor β integrals for the corresponding bonds. A similar modeling was applied recently by Ban and Kaneko[22] to study the *cis-trans* isomerization.

The Hamiltonian used for our calculation has been derived from Eq. (2.6) by omitting the diagonal term and the relaxation term. The β integrals used for the *cis-trans* isomer is given in Table I, which lists our results on the energy levels in a $(CH)_{30}$ chain. It is seen that the changes of the orbital energies are very small. Of course, a larger deviation in the β's would lead to a larger change in the energy levels. However, such values are very unlikely from the quantum-chemical point of view.

TABLE I. Orbital energy levels in (eV) of a $(CH)_{30}$ chain in different isomerizations.

	All *trans*[a]	One *cis* segment	*cis*-transoid[b]
ε_1	0.852	0.859	0.873
ε_2	1.233	1.230	1.242

[a] $\beta_< = -2.65$ eV, $\beta_> = 3.35$ eV.
[b] $\beta_< = -2.60$ eV, $\beta_> = -3.33$ eV.

Transition moments are much more sensitive to the orientation changes in the chain than on the changes of β integrals. If, for example, only a single *cis* segment is incorporated, without any constraint of the crystalline lattice, it causes a change in the orientation of the chain and, for this reason, a significant change in the transition moment ρ. However, the absolute value of ρ, which is usually of primary interest, is given by

$$|\rho| = (\rho_1^2+\rho_2^2+|\rho_1||\rho_2|)^{1/2} \tag{3.2}$$

if the bending angle is taken 60° as is the case for the nonalternating geometry [$\rho=\rho_1+\rho_2$ and the (ρ_1,ρ_2) angle is 120°]. The $|\rho|$ of Eq. (3.2) reaches its minimum value at $|\rho_1| = |\rho_2| = |\rho_0|/2$, where ρ_0 is the transition moment for the *trans* geometry. In this case we find

$$|\rho| = \frac{\sqrt{3}}{2}|\rho_0| \ .$$

Thus, this effect can decrease the transition moments, at most, by a factor of 0.8. More than one remnant *cis* segment can, however, significantly alter the geometry and the value of the transition moment. Although, as indicated by the third column of Table I, the *cis-trans* isomer is very similar to the all-*trans* one in this primitive model. We note that the experimental results on the first transition energy for *cis*-$(CH)_x$ are rather uncertain. An all-valence-electron SCF calculation on the role of a remnant *cis* segment will be reported for in Sec. III G.

D. Chain bending

The in-plane bending of the polyene chain does not affect the matrix elements of the Hückel Hamiltonian in the first-neighbor approximation, similar to the case of *cis-trans* isomerization. Thus we have investigated the possibility of introducing second-neighbor matrix elements to describe such geometry changes, but no significant effect was found for the electronic energies. The transition moments do change even in the first-neighbor approximation where the wave function and the transition energies remain the same. A bending with an angle θ yields

$$\rho^2=\rho_1^2+\rho_2^2+2\rho_1\rho_2\cos\theta \ ,$$

where the original transition moment is $\rho_0=\rho_1+\rho_2$. So, one expects a small decrease of the transition moments upon bending and also a small component of ρ perpendicular to the chain. For reasonably small bending angles, however, both effects are indeed small and unimportant.

E. Local impurities

Local impurities on the chain, e.g., heteroatoms or side groups not affecting the hybridization state of the corresponding carbon, can be modeled by the Hamiltonian of Eq. (2.6) omitting the relaxation term and using $\varphi_\mu=0$ for all μ, but using different values for α at the perturbed centers. Such modeling of impurities is widely applied in the literature.[23] The substitution of a hydrogen atom by a CH_3 methyl group or the substitution of a carbon by an sp^2 nitrogen can, e.g., be modeled in this way. In the latter case the parameter α describes the difference between the carbon and substituent $2p_z$ orbital energies. In the former case the electron donor or acceptor nature of the side group is simulated by changing the carbon $2p_z$-orbital energy.

To study the role of an impurity on the transition energies and intensities, we considered first a $(CH)_{80}$ chain and we took $\alpha_{40}=0$, 5, and 10 eV, respectively, while α_μ for $\mu\neq 40$ is kept zero. The result is shown by Table II. It is seen that the energy of the first transition decreases with increasing α, so such modeling of local impurities does not seem to be responsible for interrupting the conjugation. It is of interest to note, however, that while the intensities of vertical transitions strongly decrease with increasing α, the off-diagonal transitions $1\rightarrow 2^*$ and $2\rightarrow 1^*$, which are completely forbidden for $\alpha=0$, become the dominant ones if a strong impurity is present. This is also indicated by Table III, which shows that significant off-diagonal transition moments may appear in a long chain even for $\alpha=2$ eV. We should point out that in the acceptable range of α values, $\alpha \lesssim 5$ eV, one cannot speak about true "localized impurity level" because the highest occupied orbital is only slightly perturbed from the one corresponding to $\alpha=0$. We can therefore conclude that the interruption of conjugation observed experimentally has nothing to do with the presence of local impurities of this type on the chain.

TABLE II. Changes in transition energies ΔE (in eV) and transition moments ρ due to a local impurity of strength α (in eV).

Transition		$\alpha=0$	$\alpha=5$	$\alpha=10$
1-1*	ΔE	1.46	1.32	1.15
	ρ	2.73	1.71	1.04
2-2*	ΔE	1.63	1.64	1.64
	ρ	2.22	1.59	1.01
1-2*	ΔE	1.55	1.37	1.19
	ρ	0.0	1.08	1.23
2-1*	ΔE	1.55	1.59	1.59
	ρ	0.0	1.60	2.08

TABLE III. Diagonal and off-diagonal transition moments in a $(CH)_{100}$ chain in the absence and in the presence of an impurity of 2 eV in the middle of the chain.

$\alpha=0$ eV	1*	2*	3*	$\alpha=2$ eV	1*	2*	3*
1	2.8	0	0	1	2.4	0.8	0.8
2	0	2.4	0	2	1.0	2.2	0.3
3	0	0	2.0	3	0.9	0.7	1.6

F. Side groups and crosslinks

Side groups not affecting the bond-length alternation and conjugation seriously, such as methyl substituents, can be modeled at the Hückel level as described in the preceding subsection. Side groups linked by a double bond to the chain, such as the carbonyl (—C=O) group, or crosslinks via a double C=C bond which does not change the sp^2 configuration of the carbons, should be considered as contributing additional electrons and orbitals. They can be described by the straightforward extension of the Hamiltonian of Eq. (2.6) and the appropriate changes of the parameters.

To study the effect of C=O groups on a long polyene chain we have performed a series of calculations for a $(CH)_{100}$ chain containing 10 carbonyl side groups at randomly selected places. The result is shown in Fig. 8 in a way similar to that demonstrated in Fig. 5 for the randomly distributed twists. As a general tendency, transition energies increase while transition moments decrease due to the carbonyls, as is typical for a partial interruption of conjugation. It is found that both the energies and intensities are rather sensitive to the distribution of the carbonyls. Transition energies can increase by 50% and the transition moments can decrease to 70%. This situation is the opposite of that observed for randomly distributed twists in a $(CH)_{100}$ chain (cf. Fig. 5), where the distribution of energies and moments is rather narrow. However, even in this case a resonance transition energy in the range of 3 eV cannot be obtained unless a considerable higher concentration of carbonyl groups is assumed along the chain.

G. All-valence-electron calculations

Other type of defects, where the inclusion of all the valence electrons is necessary, are the sp^3 configurations and the single-bond cross links. We examined the following model systems shown in Fig. 9:

Model I is a simple $(CH)_9$ chain containing an sp^3 carbon in the middle with two hydrogens below and above the molecular plane. The all-*trans* isomer is considered.

Model II is the same as model I, but one *cis* segment is assumed in the vicinity of the sp^3 carbon.

Model III consists of two chains of type of model II, linked by a crosslink at the sp^3 carbons instead of one of the hydrogens. The two chains are situated in parallel planes.

Model IV is a crosslink between two $(CH)_9$ chains with all carbons being in states sp^2. Accordingly, the chains are linked with a formal double bond.

Model V is a single $(CH)_9$ chain containing one carbonyl sidegroup in the middle.

Model VI is simply butadiene modeling the complete interruption of the conjugation in the above cases.

As to the geometry, in all the above models the following bond lengths have been used: $r_< = 1.327$ Å, $r_> = 1.477$ Å, $r_{CH} = 1.085$ Å, $r_{C=C} = 1.34$ Å, $r_{C-C} = 1.54$ Å, and $r_{C=O} = 1.22$ Å. Bond angles are standard trigonal (120°) or tetrahedral (109.47°) angles. We point out that models III and IV may not exist in the all-*trans* form because H atoms would get too close to each other in that case.

For the above models, transition energies and moments have been evaluated by the CNDO/S SCF + CI method, using the seven highest occupied and the eight lowest virtual MO's in the CI calculation. Thus our excited-state

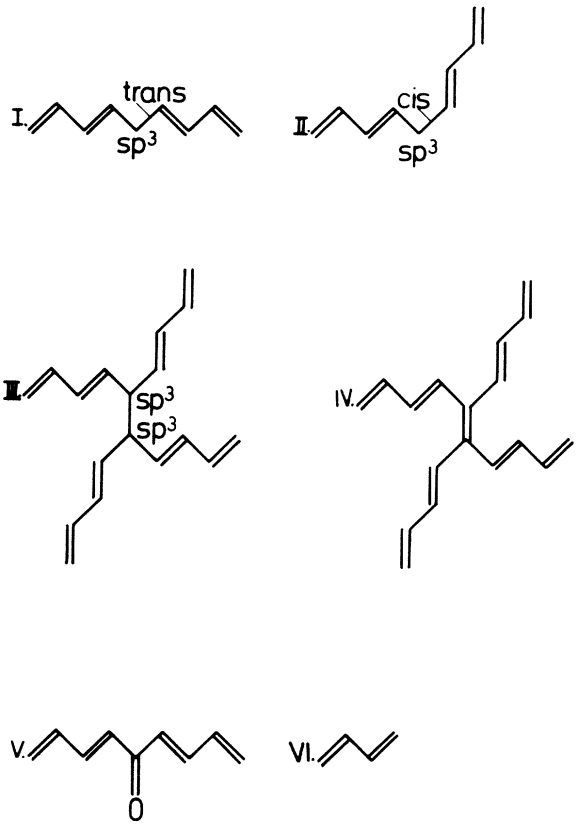

FIG. 9. Model systems to study chain defects and crosslinks in polyacetylene.

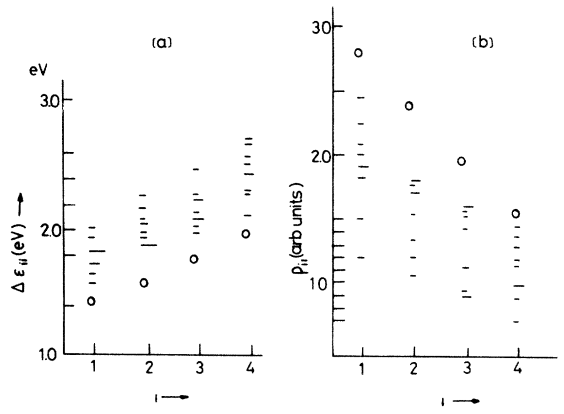

FIG. 8. Probability histogram for the effect of ten carbonyl side groups at statistically distributed places in a $(CH)_{100}$ chain. For notations, see Fig. 5.

TABLE IV. Transition energies and transition moments for models I–VI, as obtained by the CNDO/S-CI method.

	I	II	III	IV	V	VI
ΔE_1	5.48	5.52	5.41	3.15	4.99	6.04
ΔE_2	5.78	5.82	5.49	4.44		
ΔE_3	6.27	6.09	5.65	4.47	6.20	
ΔE_4	6.35	6.18	5.74		6.34	
ρ_1	1.82	1.42	2.04	1.56	1.82	1.33
ρ_2	0.22	0.82	1.36	0.59		
ρ_3	0.70	0.84	0.74	0.22	0.88	
ρ_4	0.27	0.80	0.78		0.47	

wave function is a linear combination of 56 singly excited configurations.

The results of the calculation are compiled in Table IV. By comparing models I and II, we can see that *cis-trans* isomerization at one segment does not affect the transition energies too strongly, especially for the lowest excitations. The decrease of the first transition moment from 1.82 to 1.42 is mainly a consequence of the change in the orientation of the chain due to the *cis* segment. In fact, the value of 1.42 is in a good agreement with the estimation based on Eq. (3.2), which gives us $\rho=1.58$ for the *cis* segment being in the middle. The small difference is to be attributed to non-nearest-neighbor effects, the mixture between σ and π orbitals, and the mixing of configurations in the CI calculations. The minor role of the *cis* segment found by the more sophisticated CNDO/S-CI calculations supports the conclusions based on the Hückel-type approach of Sec. III C.

The difference between the spectrum of the model III and those of models I and II is significant but not drastic. The energies of the transitions decrease slightly while the transition moments increase. This is because the conjugation is not completely interrupted at the sp^3 carbons: hyperconjugation effects permit the two-chain to interact, leading to an extension of the "effective" size of conjugation.

The situation is very different in the case of crosslinks *via* double bonds (model IV). They cause a strong red shift of all transitions. Clearly, this effect is due to the extension of the conjugation transmitted by the short carbon-carbon double bond as a crosslink. The absence of such intense low-energy transitions in the experimental spectrum of $(CH)_x$ is evidence for the lack of such crosslinks in the samples.

It is not difficult to correlate the transitions of model V with those of model I. The second transition of the latter is absent from the spectrum of the former, which has a completely planar structure excluding the possibility of any σ-π mixing. For the first π-π^* transition only a small red shift is observed (from 5.48 to 4.99 eV) due to the stronger conjugation at the carbonyl moiety.

Model VI is useful for comparison with the transitions of lowest energy of the other compounds. We see that the interruption of the conjugation is far from being complete in the case of models I–V, the largest transition energy (5.52 eV for model II) being still less by 0.52 eV than that of butadiene (6.04 eV) corresponding to a complete interruption.

IV. DISCUSSION OF THE RESULTS

The comparison of the calculations at the Hückel level and at the all-valence-electron level shows that the former gives good insight into the physical and chemical behavior of defects accommodated along the chain, except for extreme geometrical distortions and for geometries for which a Hückel calculation is not adequate. Thus, such results can be used to check on the possibilities of explaining the dispersion effect of Raman lines by distributed defects of the conjugation.

The general trend is that even a small defect like a twist around a single bond with a small angle leads to an increase of the optical transition energies and thus to similar effects as known for an interruption of the chain. However, some of these perturbations, like the weak twist, the bending, or the trapped *cis* segments, are quite small and can be ruled out as a basic origin for the dispersion. Even stronger perturbations, like large twists, sp^3 carbons, or double-bonded side groups, yield only small increases in transition energies if they are distributed on chains of the order of 100 carbons. This may be due to the fact that an interruption of a long chain yields two still long chains. The role of a single sp^3 is remarkable. Though it is a point defect on a one-dimensional chain, it interrupts the conjugation only to about 64% if the optical transition energies of butadiene, octatetrene, and the corresponding chain containing an sp^3 carbon are considered.

Accumulated defects turn out to yield a stronger change in the electronic structure. However, a concentration of 10% turns out to be not large enough to establish resonance conditions in the range of 3 eV on a long chain. For the 60° twists a concentration of 20% would rather be appropriate. Carbonyl groups have a stronger effect on the electronic structure, but even here a concentration between 15% and 20% is required for a reasonable opening of the gap.

This result has to be compared with the analysis of experiments from Raman scattering. For very-high-quality samples the distribution of conjugation lengths shows that 85% of the polymer is in segments with $N \geq 20$ double

bonds, which means a gap smaller than 1.8 eV.[24] Thus, according to the results presented, this part of the polymer can be described by chains with a dilute distribution of defects. For the remaining 15% of the material the distribution of conjugation lengths peaks at 10 double bonds, corresponding to an optical transition energy of 2.3 eV. Thus a certain amount of very short chains or domains of high defect accumulation must exist in *trans*-polyacetylene. This is in agreement with the analysis of the Raman results which recovered a bimodal distribution for the conjugation lengths.[4–6,24–26]

ACKNOWLEDGMENTS

The authors are very indebted to A. Vibók for help in performing some of the numerical calculations, as well as to Dr. K. Iwahana and Dr. A. Karpfen for valuable discussions. This work was supported by the Stiftung Volkswagenwerk.

[1(a)]See, e.g., Proceedings of the International Conference on Synthetic Metals [Mol. Cryst. Liq. Cryst. **117-122** (1985)]; J. Simon and J.-J. André, *Molecular Semiconductors* (Springer, Berlin, 1985). (b) J. C. W. Chien, *Polyacetylene* (Academic, Orlando, 1984), p. 88; T. Akaishi, K. Miyasaka, K. Ishikawa, H. Shirakawa, and S. Ikeda, J. Polym. Phys. Ed. **18**, 745 (1980).

[2]H. Kuzmany, Phys. Status Solidi B **97**, 521 (1980).

[3]S. Lefrant, L. S. Lichtman, H. Tempkin, and D. B. Fichten, Solid State Commun. **29**, 191 (1979).

[4]H. Kuzmany, E. A. Imhoff, D. B. Fichten, and A. Sarhangi, Phys. Rev. B **26**, 7109 (1982).

[5]G. P. Brivio and E. Mulazzi, Chem. Phys. Lett. **95**, 555 (1983).

[6]H. Kuzmany, Pure Appl. Chem. **57**, 235 (1985).

[7]P. R. Surján, A. Vibók, H. Kuzmany, and K. Iwahana, in *Proceedings of the International Winter School on Electronic Properties of Polymers, Kirchberg, Austria,* No. 63 of *Springer Series of Solid State Sciences,* edited by H. Kuzmany, M. Mehring, and S. Roth (Springer, Berlin, 1985).

[8]J. C. Slater, Phys. Rev. **36**, 57 (1930).

[9]H. C. Longuett-Higgins and L. Salem, Proc. R. Soc. London, Ser. A **251**, 172 (1959).

[10]W. P. Su, J. R. Schrieffer, and A. J. Heeger, Phys. Rev. Lett. **42**, 1698 (1979); **22**, 2099 (1980); **28**, 1138(E) (1983).

[11]M. Kertész and P. R. Surján, Solid State Commun. **39**, 611 (1981).

[12]M. Kertész, P. R. Surján, and K. Holczer, Mol. Cryst. Liq. Cryst. **77**, 341 (1981).

[13]R. L. Ellis, G. Kuehnlenz, and H. H. Jaffé, Theor. Chim. Acta **26**, 131 (1972).

[14]Z. G. Soos, Isr. J. Chem. **23**, 37 (1983); Z. G. Soos and S. Ramasesha, Phys. Rev. B **29**, 5410 (1984); S. Ramasesha and Z. G. Soos, J. Chem. Phys. **80**, 3278 (1984); Synth. Met. **9**, 283 (1984); S. Stafström and K. A. Chao, Phys. Rev. B **30**, 2098 (1984).

[15]K. Nishimoto and N. Mataga, Z. Phys. Chem. **12**, 335 (1957).

[16]R. Pariser and R. G. Parr, J. Chem. Phys. **21**, 466 (1953); **21**, 767 (1953); J. A. Pople, Trans. Faraday Soc. **49**, 1375 (1953).

[17]H. H. Jaffé, in *Semiempirical Methods in Electronic Structure Calculation,* edited by G. A. Segal (Plenum, New York, 1977).

[18]H. Kuzmany, P. R. Surján, and M. Kertész, Solid State Commun. **48**, 243 (1983).

[19]J. E. Douglas, B. S. Rabinovitch, and F. S. Looney, J. Chem. Phys. **23**, 315 (1965).

[20]H. W. Gibson, R. J. Weagley, R. A. Mosher, S. Kaplan, W. M. Prest, Jr., and A. J. Epstein, Phys. Rev. B **31**, 2338 (1985).

[21]A. Karpfen and R. Höller, Solid State Commun. **37**, 179 (1981).

[22]E. Ban and T. Kaneko, Solid State Commun. **52**, 355 (1984).

[23]A. Streitwieser, Jr., *Molecular Orbital Theory for Organic Chemists* (Wiley, New York, 1961); J. P. Albert and C. Jouanin, J. Phys. (Paris) Colloq. **44**, C3-387 (1983); D. Baeriswyl, *ibid.* **44**, C3-381 (1983).

[24]H. Kuzmany and P. Knoll, Mol. Cryst. Liq. Cryst. **117**, 385 (1985).

[25]H. Kuzmany and P. Knoll, in *Proceedings of the International-Winter School on Electronic Properties of Polymers, Kirchberg, Austria,* Ref. 7.

[26]G. P. Brivio and E. Mulazzi, Phys. Rev. B **30**, 876 (1984).